International Journal of Energy and Environmental Engineering
a SpringerOpen Journal

ORIGINAL RESEARCH Open Access

Investigation of the effect of organic working fluids on thermodynamic performance of combined cycle Stirling-ORC

Mohammad Bahrami[1*], Ali A Hamidi[2] and Soheil Porkhial[3]

Abstract

This paper presents thermodynamic investigation and environmental consideration of combined Stirling-organic Rankine cycle (ORC) power cycle. Combined cycle can be assisted by solar energy and an ORC used as an annular cold-side heat rejector for a free piston Stirling cycle. ORC can increase the power output efficiency by 4% to 8% compared to that of a Stirling standard cycle. Operating temperatures of ORC are between 80°C and 140°C. The main objective of this work is to model the combined cycle for performance optimization in respect to the use of several different working fluids with relevant temperature ranges. Total power efficiency in the range of 34% to 42% was observed for different cases. Several working fluids in the ORC were investigated from a thermal, operational, and environmental point of view. Working fluids considered were FC72, FC87, HFE7100, HFE7000, Novec649, *n*-pentane, *n*-decane, R245fa, and toluene. Practical issues like thermodynamic cycle efficiency, latent heat, density, toxicity, flammability, ozone depletion potential, global warming potential, and atmospheric lifetime are considered. Considering the cycle efficiency, *n*-decane shows the best performance at both levels of temperature supposed. However, this fluid has the highest saturated vapor specific volume (resulting in a larger condenser) and the lowest condenser saturation pressure (higher infiltration of non-condensable gases). The best candidates for the cycle regarding all the considered aspects were found to be toluene, HFE7100, and *n*-pentane. Comparing these three fluids, toluene presents the highest efficiency, the highest impact on the environment, the biggest vapor specific volume, and the minimum mass flow rate in Rankine cycle, therefore decreasing the pump power consumption. *N*-pentane exhibits the lowest cycle efficiency and vapor specific volume, but this fluid has super-atmospheric saturation pressure advantage. HFE7100 is a good working fluid from environmental and safety point of view.

Keywords: Thermodynamic investigation, Organic working fluid, Combined cycle Stirling-ORC, Environmental consideration

Background

The quest to reduce environmental impacts of conventional energy resources and, more importantly, to meet the growing energy demand of the global population had motivated considerable research attention in a wide range of environmental and engineering application of renewable form of energy 1]. The need to preserve fossil fuels and the use of renewable energies have led to the use of Stirling engines which have excellent theoretical efficiency, equivalent to the related Carnot cycle. They can consume any source of thermal energy (combustion energy, solar energy, etc.) and result in less pollution than the traditional engines [2]. High heat conversion efficiency, reliability, low noise operation, and ability of Stirling engines to use many fuels meet the demand of the effective use of energy and environmental preservation [3,4]. In most instances, the engines operate with hotter and cooler temperatures of 923 and 338 K, respectively. Engine efficiency ranges from about 30% to 40%, resulting from a typical hotter temperature range of 923 to 1073 K and normal operating speed range of 2,000 to 4,000 rpm [5].

* Correspondence: mohamad.bahramee@gmail.com
[1]Department of Energy Engineering, Graduate School of the Environment and Energy, Science and Research Branch, Islamic Azad University, Tehran 1341766394, Iran
Full list of author information is available at the end of the article

Springer

© 2013 Bahrami et al.; licensee Springer. This is an Open Access article distributed under the terms of the Creative Commons Attribution License (http://creativecommons.org/licenses/by/2.0), which permits unrestricted use, distribution, and reproduction in any medium, provided the original work is properly cited.

Generally, Stirling cycle development has focused on two areas of improvement: reducing losses and increasing power output. The proposed method of Ingram and Peterson [6] had an improvement on Stirling system performance. The total power output may be improved with the proper implementation of a combined power cycle with a bottoming organic Rankine cycle (ORC).

There is a sufficient amount of heat and availability to run a bottoming cycle from the rejected heat of a Stirling engine. Since the Stirling cycle under consideration in this study already makes use of a cooling loop as shown in Figure 1, a Rankine cycle may be readily integrated into the design in place of the cooling loop as shown in Figure 2. The proposed system [6] investigates the theoretical conditions that create maximum power output from a combined Stirling-Rankine cycle by increasing the Stirling heat rejection temperature. This reduces the power produced from the Stirling cycle itself but allows for more total power with an efficient low-temperature Rankine cycle. Rankine cycle expanders have traditionally had to be large for any attractive efficiency level. The measured isentropic efficiency of the scroll expander reaches 84% when the pressure ratio is close to the scroll intrinsic expansion ratio [7]. However, in experimental testing, the generator and scroll expanders produced 2.07 and 2.96 kW

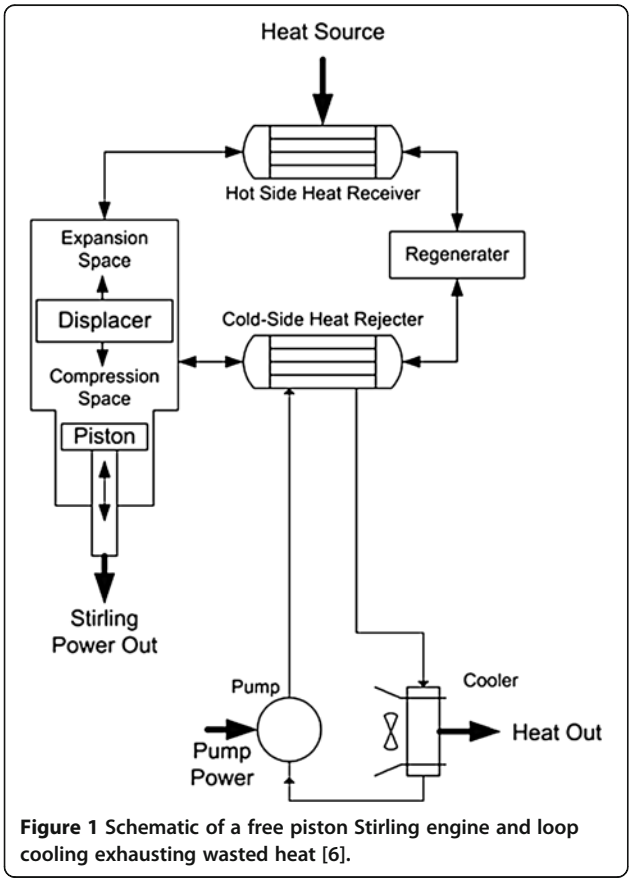

Figure 1 Schematic of a free piston Stirling engine and loop cooling exhausting wasted heat [6].

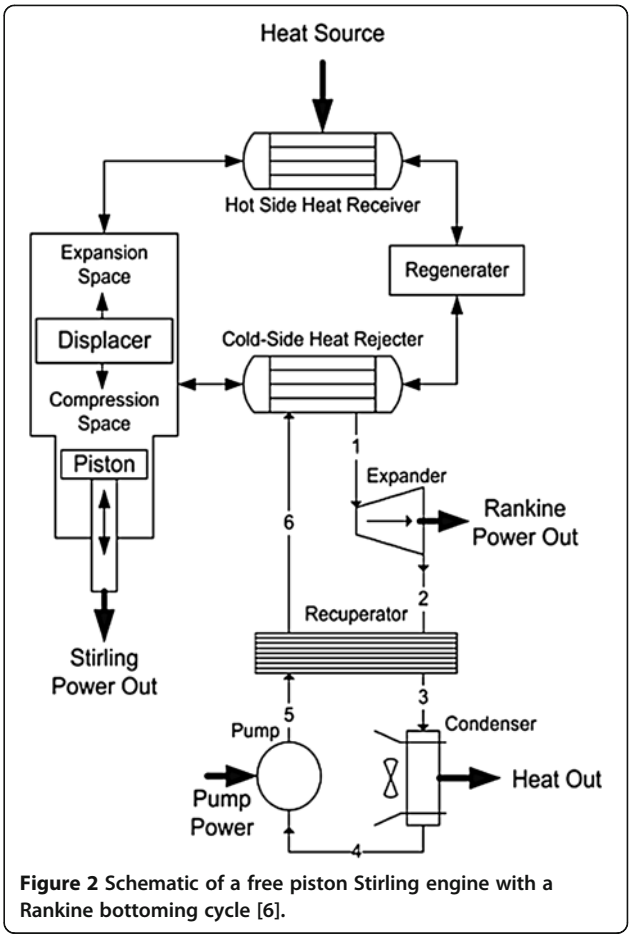

Figure 2 Schematic of a free piston Stirling engine with a Rankine bottoming cycle [6].

and had isentropic efficiencies of 0.85 and 0.83, respectively [8]. Turbine expanders sized for 1.5 kW operated with 85% isentropic efficiency [9]. The Rankine recuperator recovers heat that would otherwise be rejected from the cycle in the condenser. It is possible to use a microchannel recuperator with actual heat transfer effectiveness significantly higher than 0.85 [10]. For the sake of simplicity, the pressure drop of the recuperator is ignored.

ORC generates power from low-grade heat sources by replacing water with organic working fluids such as refrigerants or hydrocarbons [11]. To investigate any improvement when using these fluids, the effects of the properties of nine different working fluids on the overall combined cycle efficiency have been considered. In this respect, the economic, environmental, and operating performances of an ORC depend on the properties of the working fluids as well as the design and operating characteristics of the cycle. A suitable fluid for an ORC must exhibit favorable physical, chemical, environmental, safety, and economic properties such as low specific volume, liquid specific heat, viscosity, toxicity, flammability, ozone depletion potential (ODP), global warming potential (GWP), and cost, as well as favorable process characteristics

such as high efficiency, latent heat, density, molecular weight, Mollier diagram close to isentropic, suitable thermal stability limits, compatible with turbine materials and lubricating oil, non-corrosive, non-inflammable, and moderate pressure in the heat exchangers [11-13]. The saturated vapor specific volume gives an indication of condenser size, which is related to the system's initial cost. A super-atmospheric (>100 kPa) saturation pressure eliminates infiltration of gases, which is important for operational reasons, since gas infiltration reduces system efficiency. The working fluid having high latent heat and high density is preferred. To achieve the maximum output power of the combined cycle, Rankine cycle efficiency must be increased. For this reason, the effects of the properties of several working fluids on the Rankine cycle efficiency have been studied.

Among all possible alternative energy options, for example, wave energy, geothermal energy, solar energy, wind energy, and hydro energy, solar energy is becoming more popular in the world. This is mainly due to the availability of plenty of sunlight in many countries [14]. Therefore, in this study, the combined cycle is assisted by solar energy, and nine working fluids have been chosen as candidates for the bottoming ORC. These are FC72, FC87, HFE7100, HFE7000, Novec649, *n*-pentane, *n*-decane, R245fa, and toluene. Two levels of operating temperatures of ORC were considered, namely 80°C and 140°C. The solar dish used with 700°C receiver temperature was considered as the heat source. Results are presented per kilowatt of heat input to the system. Therefore, a 40% total system efficiency means 0.4-kW output power.

Methods

Working fluid classification

A working fluid can be classified as dry, isentropic, or wet fluid depending on the slope of the saturation vapor curve on a T-s diagram. Vapor saturation curve of wet fluid (e.g., water) has a negative slope, resulting in a two-phase mixture upon isentropic expansion. A dry fluid (e.g., *n*-pentane) has a positive slope, while an isentropic (e.g., R245fa) has an infinitely large slope, the fact that the vapor saturation line on a T-s diagram is vertical for these fluids [12].

Water is a suitable working fluid for the larger scale fossil fuel-fired Rankine cycle plants. Water is appropriate for those high temperature applications, but it has its limitations that become more significant during lower temperature operations. Organic fluids are generally extracted from petroleum. The main difference between organic fluids and water is the lower evaporation energy of the former, and therefore less heat is needed to evaporate the organic fluid. The thermodynamic and chemical characteristics of these fluids no longer require superheating. For most of organic fluids, an isentropic expansion from saturated vapor results in superheated vapor through a turbine at low and moderate temperatures, rather than a two-phase mixture as with water, hence avoiding complications to the turbine and cycle design [13,15]. These characteristic curves are shown in Figure 3 for the three types of fluids. The degree to which organic fluids are dry is generally related to their molecular weight or molecular complexity. For organic fluids, the larger the molecular weight, the greater is the slope of the T-s curve.

Practical issues relating to the operation and maintenance of the cycle should also be taken into account. Maizza and Maizza [16] suggested that high latent heat, high density, and low liquid specific heat are preferable. A fluid with a high latent heat and density absorbs more energy from the source in the evaporator, thus reduces the required fluid flow rate, resulting in reduced size of the facility and the pump power consumption [12]. The saturated vapor specific volume gives an indication of condenser size, which is related to system initial cost. Figures 4 and 5 respectively present the saturation pressure and vapor specific volume as a function of saturation temperature of the organic fluids considered in the analysis. It should be noted that organic fluid vapor volume varies four orders of magnitude between FC87 and *n*-decane. Organic fluids with low saturation volumes require smaller condensing equipment. Therefore, fluids with high saturation volumes are not suitable for application due to the large size of the required condensing equipment [13].

Regarding saturation pressures, it should be noted that R245fa, FC87, HFE7000, and *n*-pentane operate at super-atmospheric pressure at 40°C (condenser temperature). Super-atmospheric operation is profitable for small-scale applications by eliminating infiltration of non-condensable gases. The two main devices that are used to eliminate the non-condensable gases with a cycle operating with

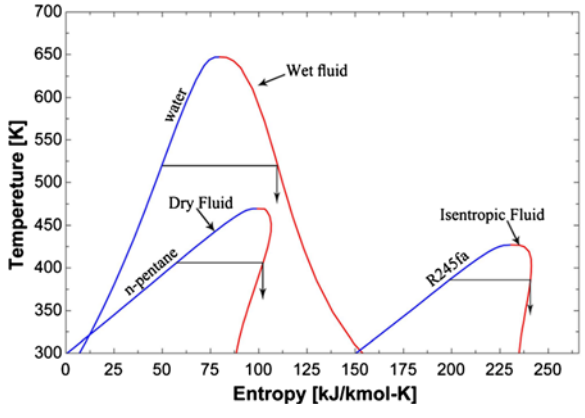

Figure 3 Three types of working fluids: dry, isentropic, and wet.

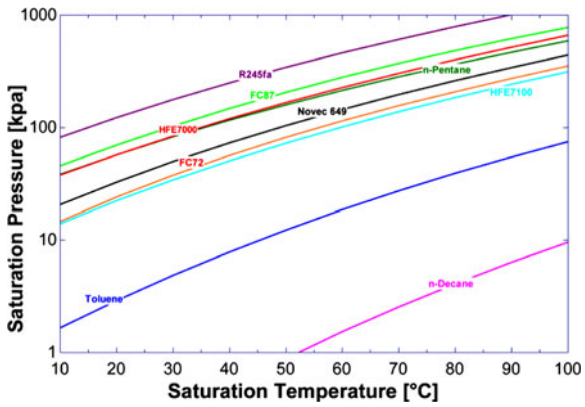

Figure 4 Saturation pressure as a function of saturation temperature.

sub-atmospheric fluids are steam jet air ejectors (SJAE) and liquid ring vacuum pumps. SJAE use high pressure motive steam to evacuate the non-condensables from the condenser (jet pump). Liquid ring vacuum pumps use a liquid compressant to compress the evacuated non-condensables and then discharge them to the atmosphere [17].

The substances that can serve as working fluids in an ORC are shown in Table 1. The table presents a classification of working fluids according to the slope of the saturation vapor line. The critical point suggests the possible operating temperature and pressure range. The molecular weight and latent heat have influence on the required mass flow rate.

Working fluid environmental impact and risk statement

The three environmental factors applicable for fluids comparison are ODP, GWP, and atmospheric lifetime (ALT). The ODP is the ratio of the impact on ozone of a chemical compared to the impact of a similar mass of R-11 or CFC-11. Thus, the ODP of R-11 is defined to be 1.0. Normally, fluids have ODPs between 0.1 and 1 [18]. GWP represents how much a given mass of a chemical contributes to global warming over a given time period as compared to the same mass of carbon dioxide. Carbon dioxide's GWP is defined as 1.0. A GWP is calculated over a specific time interval, commonly 100 years [19]. ALT is the length of time that a gas will remain in the atmosphere based on its decay rate and its tendency and likeliness to react with other gases. To complement these indices, the maximum time-average concentration for a normal 8-h work day (TOX) has also been presented as toxicological index [13,20,21].

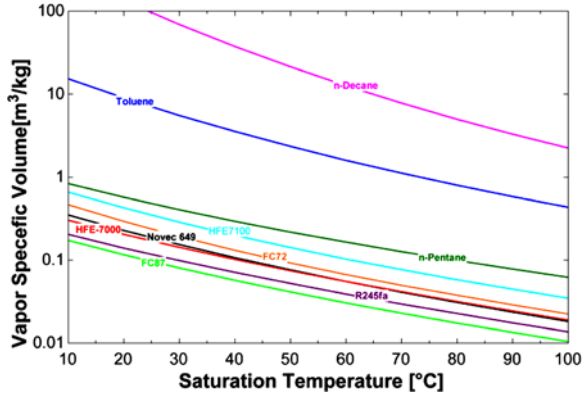

Figure 5 Saturated vapor specific volume as a function of saturation temperature.

Table 2 illustrates the environmental and safety characteristics of the working fluids under study. HFE7100, HFE7000, and Novec649 are good fluids from environmental and safety point of view. However, FC72 and FC87 perfluoro compounds (PFCs) are photo-chemically stable and are expected to persist in the atmosphere for more than 1,000 years. PFCs have high GWP, exceeding 5,000 100-year ITH. ODP for these compounds is zero [21].

Stirling-ORC combined cycle thermodynamic model description

In order to evaluate the performance of a combined cycle Stirling-ORC system, a thermodynamic model has been created. The model has been used to determine the state conditions of the working fluid in the Rankine cycle, from which the outputs from the system were analyzed.

The combined system was modeled in an idealized condition. Isentropic efficiencies were used for all components, and ideal heat exchanger effectiveness was assumed. For simplicity, the power of the fan used in the air-cooled condenser was not considered. The calculations were done at two distinct temperatures of 80°C and 140°C. The Stirling cycle was modeled as a fraction of Carnot (f_{Carnot}) thermal efficiency through Equation 1; f_{Carnot} was considered to be 0.5.

$$\eta_{\text{Stirling}} = f_{\text{Carnot}}\eta_{\text{Carnot}} \tag{1}$$

$$\eta_{\text{Carnot,St}} = 1 - \frac{T_C}{T_H}, \tag{2}$$

where, η means the efficiency, T_C is the colder temperature, and T_H is the hotter temperature. The Stirling cycle power output, W_{St}, is simply the product of the Stirling efficiency and the power into the Stirling cycle, $Q_{\text{in,St}}$. The remaining heat, $Q_{\text{out,St}}$, is rejected from the Stirling cycle and is available for the Rankine cycle.

$$W_{\text{St}} = Q_{\text{in,St}}\,\eta_{\text{St}} \tag{3}$$

$$Q_{\text{out,St}} = Q_{\text{in,St}} - W_{\text{St}}. \tag{4}$$

Table 1 Classification of working fluids according to the slope of saturation vapor line

Fluid	*P*_crit (kPa)	*T*_crit (K)	Molecular weight (g/mol)	Specific heat (J/kgK)	Latent heat (kJ/kg)	Type
FC72	1,867	448.8	338	1.100	88	Dry
FC87	2,039	421.1	228	1.100	103	Dry
HFE7000	2,478	437.7	200	1.300	142	Dry
HFE7100	2,229	468.5	250	1.183	111.6	Dry
n-decane	2,103	617.7	142.29	2.210	251.1	Dry
Novec649	1,864	441.8	316	1.103	88	Dry
n-pentane	3,364	469.7	72.15	2.363	349.00	Dry
R245fa	3,651	427.2	134.05	980.90	177.08	Isentropic
Toluene	318.6	4126	92.14	1720	399.52	Isentropic

*P*_crit, critical pressure; *T*_crit, critical temperature.

The Rankine cycle is modeled by evaluating fluid properties at state points between components. These states correspond to states 1 to 6 in Figure 2. The two cycles are connected in the model with the Stirling cycle, cold-side heat rejection being the source of heat input to the boiler of the Rankine cycle. As the ideal model is used in the study, it is assumed that all of the heat rejected from the Stirling cycle goes into the Rankine cycle. The highest Rankine cycle temperature, T_1, is 5°C below the lowest Stirling cycle temperature, and isobaric conditions are used.

$$\dot{m_{\mathrm{ORC}}}(h_1 - h_6) = Q_{\mathrm{out,St}}, \tag{5}$$

where $\dot{m}$ is the mass flow rate (g/s), and h is the specific enthalpy (J/kg). For the Rankine expander, an isentropic efficiency ($\eta_{s,\exp}$) of 0.9 was considered.

$$h_2 = h_1 - \eta_{s,\exp}\left(h_1 - h_{2,s}\right). \tag{6}$$

The recuperator is considered if the pump outlet temperature (point 5) is less than or equal to the outlet turbine temperature (point 2). For the present study, recuperator effectiveness (ε_{rec}) was assumed to be 0.9.

$$\varepsilon_{rec} = \frac{h_2 - h3}{h_2 - h(P2, T5)}, \tag{7}$$

where P is means pressure, and T is temperature. The pump is modeled with a constant isentropic efficiency of 50%, which accounts for motor efficiency and the actual isentropic efficiency of the pump [22].

$$h_5 = h_4 + \frac{1}{\eta_{s,\mathrm{pump}}}\left(h_{5,s} - h_4\right). \tag{8}$$

The model parameters represent reasonable values for physical systems and are listed with their values in Table 3.

Analysis

To evaluate the performance of the combined cycle, a numerical model was developed using thermodynamics analysis, and parametric studies were performed by

Table 2 Safety and environmental data of the working fluids

Fluid	ALT (yr)	ODP	GWP	TOX (ppm)	Risk statements
FC72	n.a.	0	n.a.	n.a.	NR
FC87	1,000	0	5,000	n.a	NR
HFE7000	4.9	0	370	75	NR
HFE7100	4.1	0	320	750	NR
n-decane	n.a.	n.a.	n.a.	1,369	HF and T
Novec649	0.014	0	1	150	NR
n-pentane	n.a.	0	20	700	EF and T
R245fa	n.a.	0	950	300	NR
Toluene	n.a.	n.a.	n.a.	100	HF and T

EF extremely flammable; *HF* highly flammable; *T* toxic; *NR* no risk statements; *n.a.* not applicable.

Table 3 Parameters for thermodynamic systems model combined Stirling-ORC power cycle

Parameter	Parameter description	Value	Units
T_{H}	Hot side temperature of Stirling cycle	700	°C
Tc	Cold side temperature of Stirling cycle	85 to 145	°C
To	Ambient temperature	25	°C
f_{Carnot}	Fraction of Carnot	0.50	
$Q_{\mathrm{in,St}}$	Heat into Stirling cycle	1	kW
$\eta_{s,\exp}$	Expander isentropic efficiency	90%	
ε_{rec}	Recuperator effectiveness	0.90	
$\eta_{s,\mathrm{pump}}$	Pump isentropic efficiency	50%	
T_{cond}	Condenser temperature	40	°C
$\Delta T_c - T_1$	Boiler temperature difference	5	°C

varying different parameters in the system. The net power output from the combined cycle is considered to be the Stirling cycle power output, W_{St}, plus the Rankine cycle expander power output, $W_{ORC,}$ less the Rankine cycle pumping power, W_{pump} (Equation 9). The total efficiency and the second law efficiency of combined cycle could be calculated through Equations 10 and 11. The Carnot efficiency is the maximum limit combined cycle efficiency and is a function of high temperature source and low temperature sink, Equation 12. The Rankine cycle and Stirling cycle efficiency could be calculated through Equations 13 and 14. The maximum power output is derived by specifying and varying particular parameters and allowing the system model to calculate all the rest. The irreversibility rate for a cycle in steady state, steady flow condition can be defined by Equation 17, where I, $T_{0,}$ S_{gen}, EX_{in}, and EX_{out} are the irreversibility, ambient temperature, the entropy generation rate in Equation 16, and the incoming and outgoing exergy flows, respectively. q_j is the heat transfer per unit mass, and Tj is the temperature of the j_{th} component of the cycle. The exergy efficiency of the combined cycle is defined by Equation 15 [23]. In fact, second law and exergy efficiency are often considered the same; in other words, the distinction between exergy and second law efficiencies is not clearly recognized by many other studies [24]. Exergy based on both useful work and useful heat are the outcomes of available energy of a thermodynamic system with respect to a reservoir. Furthermore, some studies propose a definition of exergy based on the Carnot cycle [25].

$$W_{net} = W_{St} + W_{ORC} - W_{pump} \tag{9}$$

$$\eta_{total} = \frac{W_{net}}{1kW} \tag{10}$$

$$\eta_{2law} = \frac{\eta_{total}}{\eta_{Carnot,total}} \tag{11}$$

$$\eta_{carnot,total} = 1 - \frac{T_{cond}}{T_H} \tag{12}$$

$$\eta_{ORC} = \frac{W_{ORC} - W_{pump}}{Q_{out,St}} \tag{13}$$

$$\eta_{St} = \frac{W_{St}}{Q_{in,St}} \tag{14}$$

$$\eta_{ex} = \frac{\text{Exergy recovered}}{\text{Exergy supplied}} = \frac{W_{net}}{W_{rev}} = \frac{W_{net}}{W_{net} + T_0\, S_{gen}} \tag{15}$$

$$S_{gen} = \frac{Q_{cond}}{T_{cond}} - \frac{Q_{in,St}}{T_H} \tag{16}$$

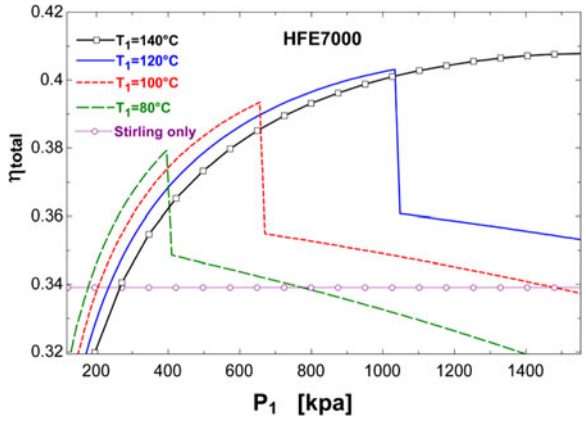

Figure 6 The total efficiency line is shown where the optimal pressure is found at each Rankine cycle operating temperature.

$$I = T_0\, S_{gen} = T_0 \sum_j \left(\frac{q_j}{T_j}\right) = EX_{in} - EX_{out} \tag{17}$$

Results and discussion

T_c is the temperature at which the Stirling cycle is rejecting heat from the cold-side heat exchanger. As this temperature rises, the maximum possible efficiency, the Carnot efficiency, from the Stirling cycle decreases. If the fraction of Carnot efficiency remains constant for the Stirling cycle, then the Stirling efficiency drops. In Rankine cycle, the turbine inlet pressure was optimized to maximize the thermal efficiency. This optimization makes it possible to decide whether it is better to have saturated vapor or superheated vapor at turbine inlet. The optimization was done with EES software [26]. The selection of the fluid for the cycle was complicated. For this cycle, where the operating temperatures are 80°C to 140°C, it is necessary to consider that all the fluids have

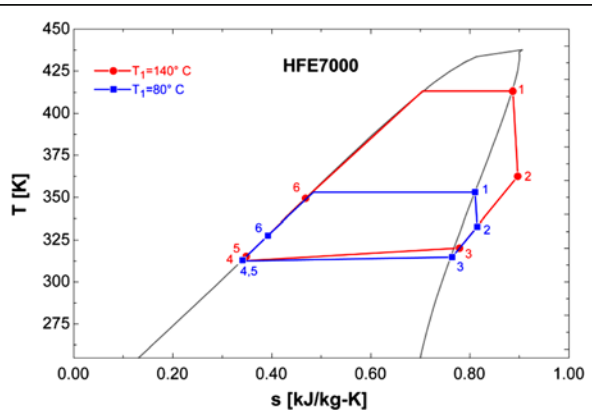

Figure 7 T-s process diagram for a Rankine cycle. Operated at maximum power conditions for the combined cycle operating temperatures of 80°C and 140°C.

Table 4 Thermal performance of several fluids in combined cycle for the ORC operating at 80°C

Fluid	P_1 (kpa)	P_2 (kpa)	V_3 (m^3/kg)	SHΔT	$Q_{out,St}$ (W)	Q_{cond} (W)	η_{ST} (%)	η_{ORC} (%)	η_{total} (%)	η_{2law} (%)	η_{ex} (%)	W_{pump} (W)	$\dot{m}$ (g/s)
FC72	208.4	56.36	0.13	0.06	684	621.3	31.6	9.16	37.87	55.83	57.04	1.42	6.78
FC87	484.8	147.7	0.06	0.07	684	623.1	31.6	8.9	37.69	55.57	56.78	3.46	6.73
HFE7000	400	119.7	0.10	0.03	684	620.3	31.6	9.31	37.97	56	57.19	2.18	4.66
HFE7100	184.6	50.48	0.20	0.05	684	619.7	31.6	9.40	38.03	56.08	57.28	1.09	5.16
n-decane	4.097	0.49	37.7	0.01	684	617.9	31.6	9.67	38.21	56.35	57.55	0.02	1.73
Novec649	261.6	72.96	0.11	0.06	684	620.9	31.6	9.22	37.91	55.89	57.1	1.87	6.72
n-pentane	366.6	116.3	0.29	0.06	684	620.3	31.6	9.3	37.97	55.98	57.18	1.43	1.73
R245fa	789.1	249.6	0.07	0.08	684	622.3	31.6	9.02	37.77	55.7	56.9	2.84	3.40
Toluene	38.41	7.907	3.55	0.53	684	618.5	31.6	9.57	38.15	56.25	57.45	0.11	1.53

P_1, inlet turbine pressure; P_2, outlet turbine pressures; V_3, specific volume at condenser inlet; $\dot{m}$, mass flow rate.

a critical temperature above 140°C. In Figure 6, for example, the total efficiency of combined cycle for HFE7000 is plotted as a function of pressure. The T_c is held constant, while pressure is varied; the system total efficiency levels are compared. Each constant T_1 line in the Figure 6 exhibits the same behavior. In other words, total efficiency increases with rising pressure until a maximum is reached, then total efficiency drops off sharply, and continues to decline as the pressure increases. The total efficiency of combined cycle eventually drops below the horizontal line representing the efficiency from the original standard Stirling system. The maximum possible total efficiency always increases with increasing pressure for the full range shown. The peaks occur when saturation conditions are reached at the Rankine boiler. The lines then drop down in power level immediately after saturation because the pressure has risen until the limited temperature is no longer sufficient to boil the fluid. Up to the point of reaching the saturation conditions, there is a decrease in the amount of superheat going into the expander with increasing pressure.

As shown in Figure 6, the combined cycle total efficiency lines do not drop below the original standard Stirling cycle efficiency until long after the saturation pressure was passed. Moving from saturated liquid to saturated vapor by boiling the Rankine fluid does not change the Stirling cycle efficiency, or Stirling power output, since it is an isothermal process. Because there is more energy in the saturated vapor, a smaller mass flow rate is required to absorb all the rejected heat from the Stirling cycle. In this way, there is less pumping power input to the system. With this fluid, there is also a much greater change in entropy expanding with a higher fraction of the fluid vaporized (higher quality). T-s process diagram in two levels of temperature for the different system state points is shown for HFE7000 in Figure 7. The states in the processes illustrated correspond to the system schematic in Figure 2.

Tables 4 and 5 present a comparison of different fluids for the Rankine cycle operating at 80°C and 140°C, respectively. The inlet and outlet turbine pressures, ΔT of superheating at point 1, specific volume at condenser inlet, rejected heat into Rankine cycle, condenser heat, Stirling cycle efficiency, Rankine cycle efficiency, total efficiency of the combined cycle, second law efficiency of the combined cycle, exergy efficiency of the combined cycle, Rankine cycle pumping power, and the mass flow rate of working fluid in the Rankine cycle have all been presented.

When operating at 80°C, *n*-decane presents the best thermal performance compared to all other fluids. This

Table 5 Thermal performance of several fluids in combined cycle for the ORC operating 140°C

Fluid	P_1 (kpa)	P_2 (kpa)	V_3 (m^3/kg)	SHΔT	$Q_{out,St}$ (W)	Q_{cond} (W)	η_{ST} (%)	η_{ORC} (%)	η_{total} (%)	η_{2law} (%)	η_{ex} (%)	W_{pump} (W)	$\dot{m}$ (g/s)
FC72	884.7	56.36	0.13	0.03	714.8	590.1	28.52	17.45	40.99	60.44	61.61	8.39	6.15
FC87	1747	147.7	0.06	0.02	714.8	606.6	28.52	15.14	39.34	58	59.19	20.86	6.18
HFE7000	1545	119.7	0.11	0.92	714.8	592.2	28.52	17.15	40.78	60.12	61.3	12.73	4.29
HFE7100	775.5	50.48	0.20	0.02	714.8	583.9	28.52	18.32	41.61	61.35	62.51	6.2	4.69
n-decane	38.82	0.5	38.18	0.02	714.8	574.8	28.52	19.59	42.52	62.7	63.84	0.17	1.58
Novec649	1072	72.96	0.11	0.02	714.8	592.6	28.52	17.11	40.74	60.08	61.25	11.07	6.09
n-pentane	1329	116.3	0.30	0.02	714.8	585.4	28.52	18.11	41.46	61.13	62.29	6.42	1.61
R245fa	2337	249.6	0.07	10.05	714.8	598.9	28.52	16.21	40.11	59.13	60.32	10.31	3.21
Toluene	218.9	7.907	3.58	0	714.8	577.4	28.52	19.22	42.26	62.31	63.45	0.70	1.42

P_1, inlet turbine pressures; P_2, outlet turbine pressures; V_3, specific volume at condenser inlet; $\dot{m}$, mass flow rate.

can be seen in Table 4. Again, when operating at 140°C, *n*-decane, with 0.02°C of superheating, presents the best combined cycle efficiency as it is illustrated in Table 5. Toluene, HFE7100, *n*-pentane, Novec649, and HFE7000 present acceptable efficiencies, but Toluene and *n*-pentane are toxic and flammable. *N*-decane requires minimum pumping power in Rankine cycle, and HFE7000 and *n*-pentane have super-atmospheric saturation pressure.

Conclusion

The main conclusion of this work is maximization of combined cycle efficiency with the choosing of suitable working fluid for ORC as bottoming cycle operating at 80°C to 140°C. It is difficult to find the best fluid, which has simultaneously high cycle efficiency, low vapor specific volume at turbine outlet, super-atmospheric saturation pressure, high latent heat, high density and low liquid specific heat, low environmental impact, low toxicity, and has non-combustion characteristics.

For the ORC operating at the two levels of temperature, *n*-decane presented the highest cycle efficiency between the dry and isentropic fluids. But this fluid presents the highest vapor specific volume, leading to a very large condenser and high initial cost. It also presents the lowest saturation pressures, leading to infiltration of non-condensable gases.

There are only four fluids with super-atmospheric saturation pressure: R245fa, FC87, HFE7000, and *n*-pentane. The best candidates for the cycle regarding all the aspects are toluene, HFE7100, and *n*-pentane. *N*-pentane does not require special sealing system because the cycle operates at super-atmospheric saturation. Toluene presents the highest vapor specific volume, the lowest saturation pressure, and the least mass flow rate, leading to the smallest size of utilities, equipments, and the pump consumption among the three fluids. From the environmental and safety point of view, HFE7100 has a small impact compared with toluene and *n*-pentane. For the system operating at 80°C, toluene presents total combined cycle efficiency of 38.15% against 38.03% of HFE7100 and 37.97% of *n*-pentane. These values of cycle efficiency are similar. For the Rankine cycle operating at 140°C, the difference in the total combined cycle efficiency is bigger. Total efficiencies for different fluids investigated are the following: toluene 42.26%, HFE7100 41.61%, and *n*-pentane 41.46%. A small efficiency leads to a high heat input in the combined cycle; therefore, a big capital investment in solar dish area is required.

Abbreviations

0: Ambient; 2law: Second law; ΔT: Temperature difference (°C); ε_{rec}: Recuperator effectiveness; η: Efficiency (%); ALT: Atmospheric lifetime (years); C: Cold side of Stirling cycle; Carnot: Carnot; cond: Condenser; crit: Critical; Ex: Exergy (W); Exp: Expander; *f*: Fraction constant; GWP: Global warming potential (100-year period); *h*: Specific enthalpy (J/kg); H: Hot side of Stirling cycle; *I*: Irreversibility (W); in: Input; *j*: Cycle component index; $\dot{m}$: Mass flow rate (g/s); net: Met output; ODP: Ozone depletion potential (CFC as a reference); ORC: Organic Rankine cycle; out: Output; *P*: Pressure (Pa); *Q*: Heat transfer rate (W); S_{gen}: Entropy generation rate (W/K); S: Isentropic; st: Stirling cycle; *T*: Temperature (°C); total: Total; W: Power (W).

Competing interest

The authors declare that they have no competing interests.

Authors' contributions

MB carried out all the computation, performed the modeling, modeling analysis, software simulation, and drafted the manuscript. AAH checked the equations and analysis, reviewed the revised manuscript, and helped in correcting the manuscript. All authors read and approved the final manuscript.

Authors' information

MB graduated the MSc in Energy Engineering in 2012 from the Sciences and Research Branch Islamic Azad University, Tehran, Iran. His current research focuses on thermodynamic cycles and refrigeration. AAH is a professor at the Chemical Engineering Department of Tehran University, Iran. He received his Ph.D. from the Department of Chemical Engineering and Fuel Technology of Sheffield University, England in 1986. Ever since returning to Iran, he has been working at Tehran University teaching heat transfer and combustion and fuel-related courses. His main research interests are heat transfer phenomena, heat exchangers design and performance, and recently, the application of nanofluids in cooling systems. He has co-authored over 70 papers published in national and international journals and conferences. He is also very active in translating and writing books (in Persian) on Chemical Engineering subjects specially on heat transfer. SP is an assistant professor at the Mechanical Engineering Department of Islamic Azad University, Karaj Branch, Iran. He received his Ph.D. from the Department of Mechanical Engineering at the Amir Kabir University of Technology, Tehran, Iran with GPA in 2002. His areas of interest include heat transfer, cooling, and renewable energy. He also teaches courses on dynamics, heat transfer, thermodynamics, and refrigeration at the Islamic Azad University, Karaj Branch. He is the head of the Iranian Geothermal Energy Agency (IGEA) and the Technology Transfer in Renewable Energy Organization (SUNA), Tehran, Iran. He has published 12 conference papers, 3 ISI papers, and 3 books.

Acknowledgments

The authors would like to express their sincere gratitude to the editor (Professor Farivar Fazelpour) and anonymous reviewers for their invaluable comments and suggestions, which substantially improved the overall quality of the manuscript. The support from the Department of Energy Engineering, Science and Research Branch, Islamic Azad University, Tehran, Iran, is gratefully acknowledged.

Author details

[1]Department of Energy Engineering, Graduate School of the Environment and Energy, Science and Research Branch, Islamic Azad University, Tehran 1341766394, Iran. [2]Department of Chemical Engineering, Tehran University, Tehran 1417613131, Iran. [3]Department of Mechanical Engineering, Islamic Azad University (Karaj Branch), Alborz, Karaj 1998833871, Iran.

Received: 20 May 2012 Accepted: 18 December 2012
Published: 26 February 2013

References

1. Sunday, O, Oyedepo, SO, Adaramola, MS, Paul, S: Analysis of wind speed data and wind energy potential in three selected locations in south-east Nigeria. IJEEE **3**, 7 (2012)
2. Timoumi, Y, Tlili, I, Ben Nasrallah, S: Performance optimization of Stirling engines. Renew. Energy **33**, 2134–2144 (2008)
3. Thombarea, DG, Verma, SK: Technological development in the Stirling cycle engines. Renew. Sustain. Energy Rev. **12**, 1–38 (2008)
4. Wei, F, Wang, R, Diguet, G, Lin, G: Performance optimization of irreversible ferromagnetic Stirling heat pumps. IJEEE **2**(2), 77–83 (2011)
5. Kongtragool, B, Wongwises, S: Thermodynamic analysis of a Stirling engine including dead volumes of hot space, cold space and regenerator. J. Renew. Energy **31**, 345–359 (2006)

6. Ingram-Goble, R, Peterson, R: Modeling and optimization of a combined cycle Stirling-ORC system and design of an integrated microchannel Stirling heat rejector. Mechanical Engineering Department, Oregon State University, MSc Thesis (2010)
7. Wang, H, Peterson, R, Harada, K, Miller, E, Ingram-Goble, R, Fisher, L, Yih, J, Ward, C: Performance of a combined organic Rankine cycle and vapor compression cycle for heat activated cooling. Energy **36**(1), 447–458 (2011)
8. Mathias, JA, Johnston, J, Cao, J, Priedeman, DK, Christensen, RN: Experimental testing of gerotor and scroll expanders used in, and energetic and exergetic modeling of, an organic Rankine cycle. J. Energ. Resour-ASME **131**, 012201–012209 (2009)
9. Yagoub, W, Doherty, P, Riffat, S: Solar energy-gas driven micro-chip system for an office building. Appl. Therm. Eng. **26**, 1604–1610 (2006)
10. Wang, H, Peterson, RB: Performance Enhancement of a Thermally Activated Cooling System Using Microchannel Heat Exchangers. Oregon State University Corvallis, Oregon (2011)
11. Papadopoulos, A, Stijepovic, M, Linke, P: On the systematic design and selection of optimal working fluids for Organic Rankine Cycles. Appl. Therm. Eng. **30**, 760–769 (2010)
12. Chen, H, Goswami, D, Stefanakos, EK: A review of thermodynamic cycles and working fluids for the conversion of low-grade heat. Renew. Sustain. Energy Rev. **14**, 3059–3067 (2010)
13. Facão, J, Oliveira, AC: Analysis of energetic, design and operational criteria when choosing an adequate working fluid for small ORC systems. In: ASME 2009 International Mechanical Engineering Congress & Exposition, pp. 13–19. Lake Buena Vista, Florida (2009)
14. Sharma, P, Harinarayana, T: Enhancement of energy generation from two layer solar panels. IJEEE **3**, 12 (2012)
15. ORCycle: From waste heat to electricity. (2012). http://www.orcycle.be/index.php/en/orctheorie. Accessed 09 March 2012
16. Maizza, V, Maizza, A: Working fluids in non-steady flows for waste energy recovery systems. Appl. Therm. Eng. **16**, 579–90 (1996)
17. Vosough, A, Falahat, A, Vosough, S, Nasr Esfehani, H, Behjat, A, Naseri Rad, R: Improvement power plant efficiency with condenser pressure. IJMSE **2**, 38–43 (2011)
18. US Environmental Protection Agency: Ozone Layer Protection Glossary. USEPA, Washington DC (2010)
19. US Environmental Protection Agency: Global Warming Potentials of ODS Substitutes. USEPA, Washington DC (2011)
20. Facão, J, Palmero-Marrero, A, Oliveira, AC: Analysis of a solar assisted micro-cogeneration ORC system. Int. J. Low. Carbon. Tech. **3**(4), 254–264 (2008)
21. 3M: Innovative technology for a changing world. (2012). http://www.3m.com. Accessed 18 March 2012
22. Brasz, JJ: Assessment of C6F as working fluid for organic Rankine cycle applications. Paper presented at the international refrigeration and air conditioning conference, pp. 10–12. Purdue University, Columbia City (2008)
23. Rayegan, R, Tao, YX: A procedure to select working fluids for solar organic Rankine cycles (ORCs). Renew. Energy. **36**, 659–670 (2011)
24. Lior, N, Zhang, N: Energy, exergy, and second law performance criteria. Energy **32**, 281–296 (2007)
25. Palazzo, P: Thermal and mechanical aspect of entropy-exergy relationship. IJEEE **3**, 4 (2012)
26. Klein, SA: Engineering equation solver. F-chart software, McGraw Hill, New Jersey (2010)

doi:10.1186/2251-6832-4-12
Cite this article as: Bahrami *et al.*: Investigation of the effect of organic working fluids on thermodynamic performance of combined cycle Stirling-ORC. *International Journal of Energy and Environmental Engineering* 2013 **4**:12.

Submit your manuscript to a SpringerOpen journal and benefit from:

► Convenient online submission
► Rigorous peer review
► Immediate publication on acceptance
► Open access: articles freely available online
► High visibility within the field
► Retaining the copyright to your article

Submit your next manuscript at ► springeropen.com